Astron. Astrophys. 340, 129–134 (1998)

ASTRONOMY
AND
ASTROPHYSICS

RX J1016.9–4103: a new soft X-ray polar in the period gap⋆

Jochen Greiner and Robert Schwarz

Astrophysical Institute Potsdam, An der Sternwarte 16, D-14482 Potsdam, Germany

Received 18 August 1998 / Accepted 14 September 1998

Abstract. We have discovered a new AM Her system as the optical counterpart of the ROSAT All-Sky-Survey source RX J1016.9–4103 (≡ 1RXS J101659.4-410332). The X-ray spectrum is very soft and the X-ray intensity is strongly modulated with the orbital period. Optical photometric and spectroscopic follow-up observations reveal a synchronously rotating binary with an orbital period of 134 min, placing RX J1016.9–4103 in the period gap. The strength of the TiO bands suggests a secondary spectral type later than M3 V and a distance of 615±150 pc. Based on two clearly visible broad humps in the optical spectrum (interpreted as cyclotron features) a magnetic field strength of 52 MG is deduced thus proving the polar classification.

Key words: stars: individual: RXJ 1016.9-4103 – novae, cataclysmic variables – X-rays: stars

Table 1. Log of observations

Telescope[a]	Date	Energy Band	$T_{\rm int}$ (sec)
	X-ray		
ROSAT P	1990 Dec 09–11	0.1–2.4 keV	430
ROSAT P	1993 Nov 30–Dec 4	0.1–2.4 keV	6760
ROSAT P	1994 Jun 01	0.1–2.4 keV	2930
ROSAT H	1997 Dec 08	0.1–2.4 keV	1800
	optical spectroscopy		
ESO 2.2 m	1995 Mar 26	3000–9000 Å	1800
	optical photometry		
ESO 2.2 m	1995 Mar 25–27	B, R	600, 180

[a] The abbreviations have the following meanings: ROSAT P or H = PSPC or HRI detectors onboard the ROSAT satellite, ESO = European Southern Observatory, La Silla/Chile.

1. Introduction

AM Her type variables are a subgroup of cataclysmic variables (CVs) in which the magnetic field of the white dwarf controls the geometry of the material flow between the main-sequence donor and the white dwarf primary as well as synchronizes the white dwarf spin period with the binary orbital period (see e.g. Warner 1995 for a detailed review). The inflow of matter along the magnetic field lines (of one or occasionally also two magnetic poles) is decelerated above the white dwarf surface producing a shock front. This region is thought to emit hard X-rays (usually modelled in terms of thermal bremsstrahlung of 10–20 keV) and polarized cyclotron radiation (hence these systems are named also polars) in the IR to UV range. In addition, a strong soft component has been frequently observed from polars which is thought to arise from the heated accretion pole (usually modelled in terms of blackbody emission with 20–50 eV temperature).

It is this soft X-ray component which has led to the discovery of a few dozen new polars by ROSAT observations over the last 8 years, most notably the ROSAT all-sky survey (e.g. Beuermann & Burwitz 1995 for a first summary). Based on these discoveries, the strength of the soft component (or more precisely the ratio of the blackbody and the bremsstrahlung component) has been found to increase with the magnetic field strength of the white dwarf. Since simple reprocession of the hard component cannot produce the observed soft X-ray fluxes, a scenario of high-$\dot{m}$, blobby accretion has been proposed as a mechanism to explain the soft excess (Kujpers & Pringle 1982). In a different approach, bremsstrahlung emission is gradually replaced by more efficient cyclotron cooling at high magnetic field strengths (Woelk & Beuermann 1996).

The source described here has been discovered as a result of a systematic survey for supersoft X-ray sources in the all-sky survey data (see Greiner 1996 for details of this survey) which revealed a large number of CVs and single white dwarfs. Other polars identified from this sample include V844 Her = RX J1802.1+1804 (Greiner, Remillard and Motch 1995, 1998), RS Cae = RX J0453.4–4213 (Burwitz et al. 1996), and RX J1724.0+4114 (Greiner, Schwarz and Wenzel 1998). In this paper we present photometric, spectroscopic and X-ray observations (summarized in Table 1) which led to the discovery of another polar, RX J1016.9–4103 (henceforth referred to as RX J1016).

Send offprint requests to: Greiner, (jgreiner@aip.de)

⋆ Partly based on observations collected during MPI time at the 2.2 m telescope of the European Southern Observatory, La Silla, Chile.

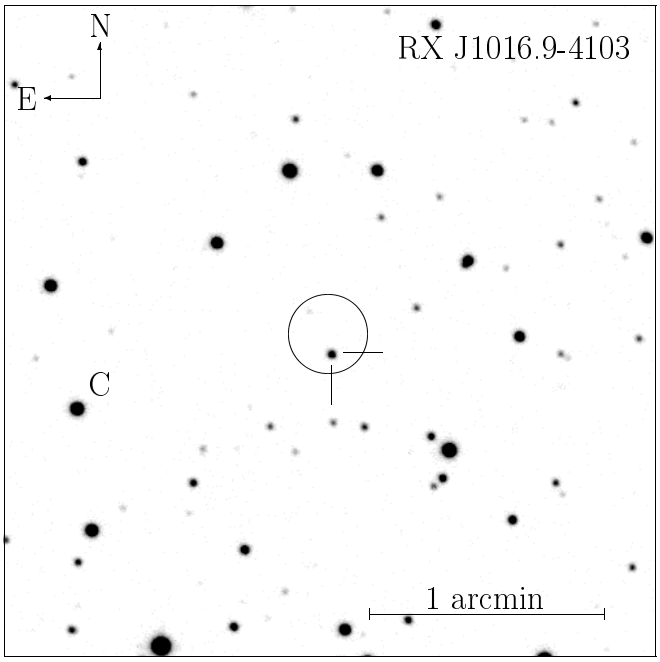

Fig. 1. A 10 min B-band CCD image of RX J1016.9–4103 obtained with the 2.2 m telescope at ESO. The circle denotes the 3σ X-ray error circle derived from the HRI pointing ($10''$ radius). The optical position is measured as: R.A. (2000.0) = $10^{\rm h}16^{\rm m}58\overset{\rm s}{.}9$, Decl. (2000.0) = $-41^\circ03'45''$ ($\pm1''$). The bright star at the left denoted with "C" has been used as comparison star for the photometry.

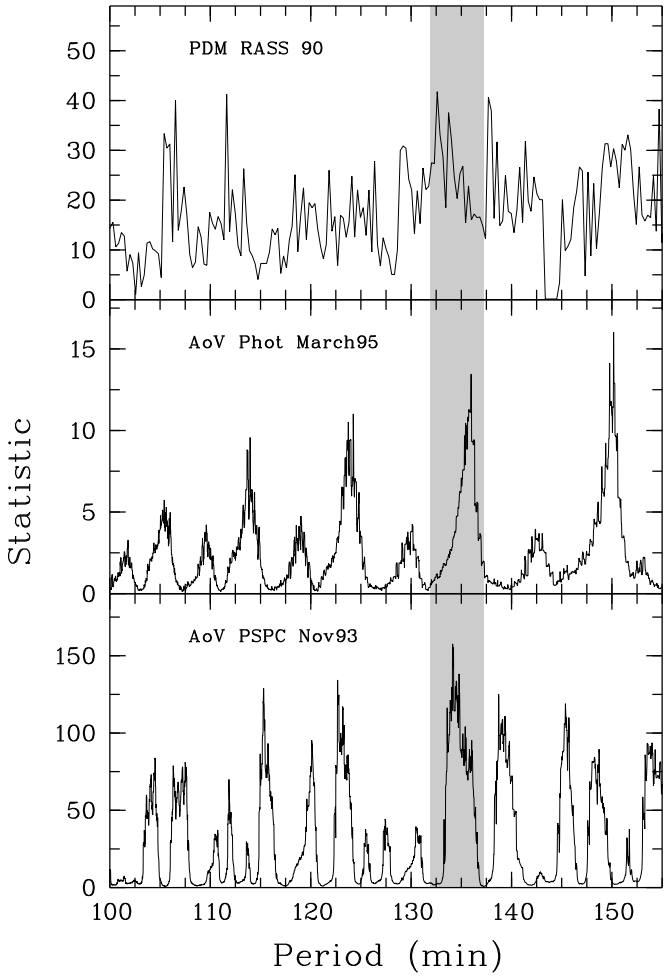

Fig. 2. Results of the period-search using the analysis-of-variance method. The adopted period of 134±3 min is marked as the shaded region.

2. X-ray discovery and identification

RX J1016 was scanned during the ROSAT all-sky-survey over a period of 4 days in December 1990 for a total observing time of 430 sec. Its mean count rate in the ROSAT position-sensitive proportional counter (PSPC) was 0.13 cts/s, and the hardness ratio $HR1 = -0.95\pm0.12$ where $HR1$ is defined as (H–S)/(H+S), with H (S) being the counts above (below) 0.4 keV over the full PSPC range of 0.1–2.4 keV.

For the timing analysis the source photons were extracted with a radius of $4'$. The background was chosen at the same ecliptic longitude at $\approx1^\circ$ distance, corresponding to background photons collected typically 15 sec before or after the time of the source photons. Standard corrections were applied using the dedicated EXSAS software package (Zimmermann et al. 1994). The RASS light curve folded over the best-fit period as derived in Sect. 3 is shown in the upper panel of Fig. 3. The X-ray flux shows 100% modulation with a peak count rate of $\sim$0.4 cts/s and a pronounced long faint-phase where the X-ray flux is nearly zero (formal count rate of 0.05 ± 0.05 cts/s).

The soft X-ray spectrum and strong variability immediately suggested the cataclysmic variable nature. Indeed, using the best-fit X-ray coordinate derived from the all-sky survey data only one optical object brighter than $20^{\rm m}$ was found within the error circle (see Fig. 1) which later was identified spectroscopically as a polar (see Sect. 4).

Dedicated follow-up pointed ROSAT observations were performed in November 30 – December 4, 1993 and June 1, 1994 with the PSPC and on December 8, 1997 with the high-resolution imager (HRI). Table 2 summarizes the relevant numbers of these measurements including the total number of detected counts (column 3), the mean count rate (column 4), the hardness ratio (column 5), the coverage of the orbital phases (column 6), the off-axis angle (column 7) and the best-fit X-ray positions (column 8).

3. Optical and X-ray variations

CCD photometry was obtained during 3 nights in March 1995 with EFOSC II at the 2.2 m telescope on La Silla (during MPI time). Observations were performed mostly with the B filter, though a few exposures also were made with the V and R filters. Exposure times ranged between 10–600 sec. Observational details are listed in Table 1. The images were processed using the profile-fitting scheme of the DoPhot reduction package (Mateo & Schechter 1989) to achieve high accuracy. The optical light curve is characterized by a broad bright phase and a shallow 0.3 mag deep faint phase. In contrast, the X-ray in-

Table 2. Basic numbers of the X-ray observations of RX J1016.9–4103

Date	Obs-ID[(1)]	N_{cts}	mean count rate (cts/s)	$HR1$	phase coverage	offaxis angle	X-ray position (equinox 2000.0)
1990 Dec 09–12[(1)]	–	57	0.13	–0.95±0.12	5%	0′–52′	$10^{\rm h}16^{\rm m}58\overset{\rm s}{.}2$ –41°03′38″ ± 15″
1993 Nov 30–Dec 4	201605p	430	0.06	–0.98±0.01	55%	0′.50	$10^{\rm h}16^{\rm m}59\overset{\rm s}{.}8$ –41°03′52″ ± 25″
1994 Jun 1	201605p-1	352	0.12	–0.98±0.01	30%	0′.32	$10^{\rm h}16^{\rm m}59\overset{\rm s}{.}2$ –41°03′44″ ± 25″
1997 Dec 08	300580h	3	0.0019[(3)]	–	20%	0′.21	$10^{\rm h}16^{\rm m}58\overset{\rm s}{.}9$ –41°03′40″ ± 10″

(1) The letters after the number denote the detector: h = HRI, p = PSPC.
(2) For the position determination only photons in the energy range 0.25–0.5 keV have been used to avoid position degradation due to ghost images.
(3) Note the lower sensitivity of the HRI at soft energies by a factor of 7.8 as compared to the PSPC.

tensity variations are much more pronounced and show a clear on/off-like behaviour.

In order to derive an orbital period we carried out a period search using the analysis-of-variance method (Schwarzenberg-Czerny 1989) for both, the optical photometry data as well as the combined ROSAT PSPC pointings and the phase-dispersion method (Stellingwerf 1978) for the ROSAT all-sky survey data. The resulting periodograms (Fig. 2) show a variety of maxima which are predominantly caused by the poor sampling rather than the intrinsic variability. A more closer look at the bottom two panels (optical and ROSAT pointing data) suggests that common periods of 123, 134 or 149 min are possible (134 min is the most reliable period from the ROSAT pointed data alone). Inclusion of the ROSAT all-sky survey data clearly favours the 134 min period though we caution that due to the orbital motion of the ROSAT satellite (96 min) the signal may be affected. We note also that the actual best-fit period of the ROSAT all-sky survey data is 132.5 min, thus being slightly smaller than the period derived from the optical and pointed ROSAT data. Note that for each data set (corresponding to the three panels in Fig. 2) a slightly different best-fit period is obtained though the errors (which we consider to correspond to the width of the peak) overlap. Overall, based on the appearance of the folded light curves (Fig. 3) according to a criterion of "greatest simplicity" we feel that $P_{\rm orb}$ = 134±3 min is our best estimate (shaded area in Fig. 2).

4. A low resolution spectrum

4.1. Optical identification

The identification spectrum of the likely counterpart was obtained on March 26, 1995 with the ESO 2.2 m telescope at La Silla/Chile and was exposed for 30 min. We used the EFOSC II spectrograph equipped with a 1k×1k Thomson CCD detector with a 450 Å/mm grism (corresponding to about 8.5 Å/pixel) covering the optical wavelength range from 3000–9000 Å. The observation was performed under stable photometric conditions and accompanied by measurements of the standard star LT4816. We additionally applied a correction using the B magnitude derived from a direct image taken just prior to the spectroscopic observation to calibrate the flux with an accuracy of $\sim$ 10% (using standard MIDAS procedures). By convolving the original spectrum with functions representing the BVR bandpasses we arrive at $B = 18\overset{\rm m}{.}3$, $V = 18\overset{\rm m}{.}5$ mag and $R = 18\overset{\rm m}{.}0$ with a mean error of ±0.2 mag for RX J1016.

The resulting spectrum plotted in the upper panel of Fig. 4 reveals strong emission lines with of the Balmer series and He II typical for a CV. The high-excitation line He II λ4686 Å is quite prominent. Its strength (2/3 of the Hβ-flux) and the inverted decrement of the Balmer lines clearly indicate a magnetic nature of the object.

4.2. The secondary star

We further deconvolved the optical spectrum by fitting a power-law in the blue range between 3800–5000 Å. After subtracting this blue continuum contribution the late-type companion is revealed by the slope of the continuum in the near–IR and obvious flux depression due to the TiO absorption throughs which are best seen in the $\lambda\lambda$ 7053 and 7667 Å bandheads. The faintness of the features prevents an accurate quantitative estimate of the spectral type, but the low ratio $\lesssim 0.5$ of the flux deficits $F_{\rm TiO}$(6165Å) to $F_{\rm TiO}$(7667Å) suggest that it is later than dM 3. The expected parameters for a Roche-lobe filling secondary in a 134 minute system are $M_2 = 0.18{\rm M}_\odot$, $R_2 = 0.22{\rm R}_\odot$ and a spectral type between M 4.5–5.5, for which the ZAMS mass-radius and mass-spectral type relations of Patterson (1984) and Kirckpatrick & McCarthy (1994) were used.

The distance of RX J1016 can be estimated from the observed strength of the M-dwarf using the method of Bailey (1981). In the following we take the dM 4.5 star Gl 83.1 ($K = 6\overset{\rm m}{.}67$) as a template and assume that both M-stars have the same colour $V - K = 5\overset{\rm m}{.}62$ (Leggett 1992). By comparing the measured flux deficits in the λ7667-band in Gl 83.1 and that of RX J1016 (1800 10^{16} and 0.2 10^{16} erg cm^{-2} s^{-1}), we derive a K magnitude of $16\overset{\rm m}{.}5$ for the secondary in RX J1016 . If we take this value and $S_K = 4.43$ from the surface brightness relationship of Beuermann & Weichhold (1998) a distance of 615 ± 150 pc is deduced. The error includes an uncertainty of 25% for both, the flux calibration and the scaling of the TiO band deficits.

Detailed phase-resolved spectroscopic studies of selected systems, e.g. AM Her (Davey & Smith 1996), QQ Vul (Schwope et al. 1998) and RX J0203.8+2959 (Schwarz et al. 1998) have

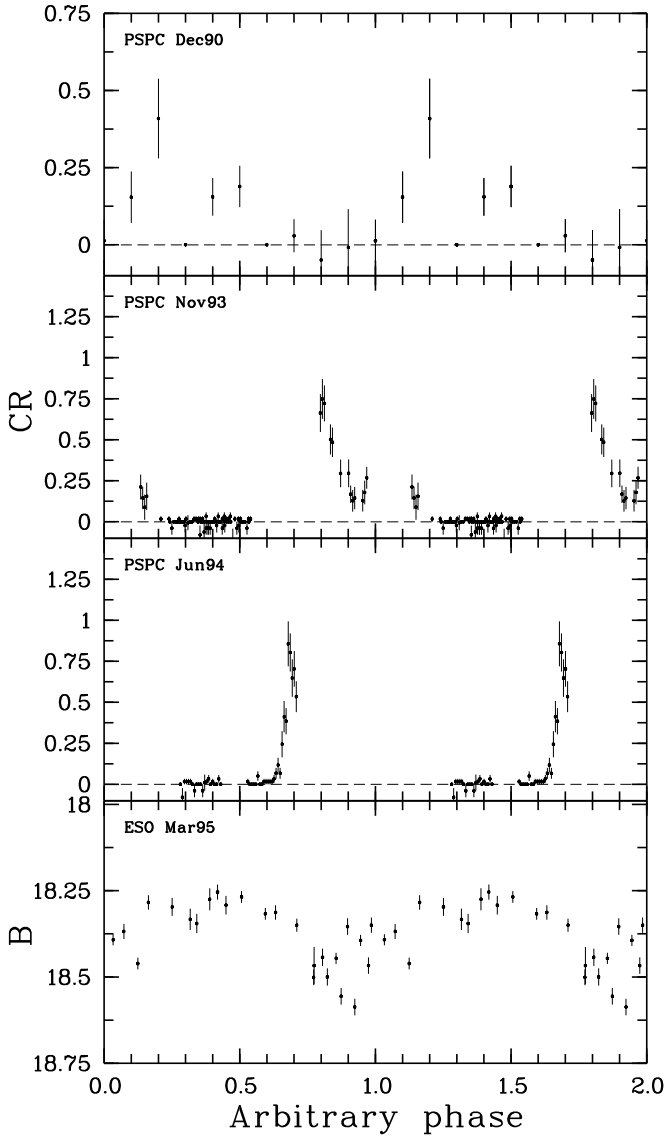

Fig. 3. Optical and X-ray light curves of RX J1016 plotted over orbital phase for a period of $P = 134.4$ min. Note that the phase designation of the middle two panels is arbitrary with respect to the all-sky survey (top panel) and optical (bottom panel) data. Data are plotted twice for clarity and units are PSPC cts/s for the upper three panels and B magnitudes for the bottom panel.

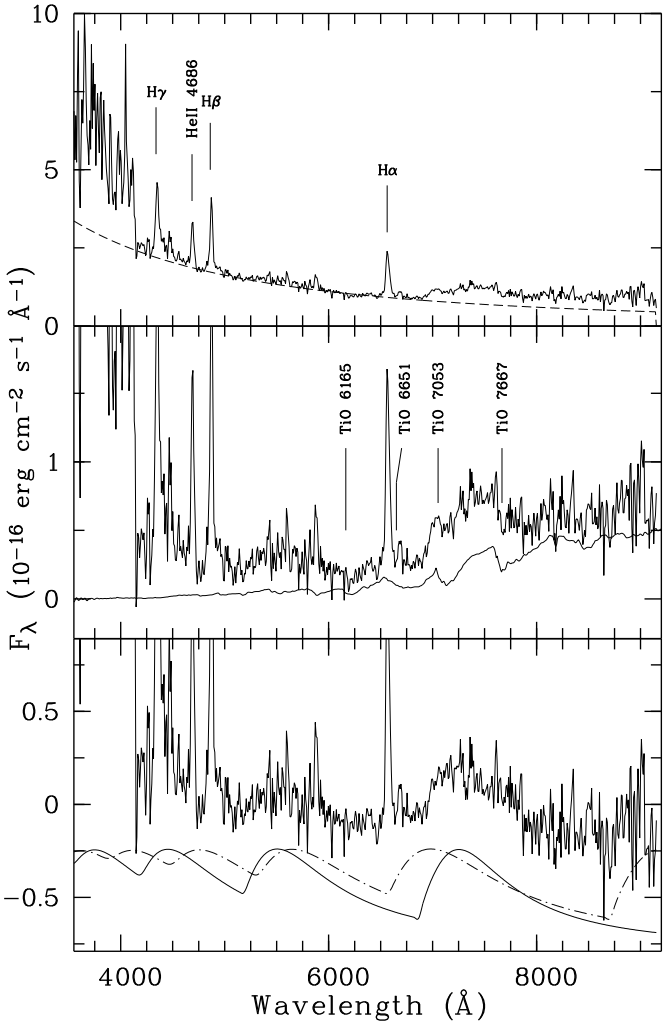

Fig. 4. upper panel: Low resolution optical spectrum of RX J1016.9–4103 obtained on March 26, 1995. The dashed line represents a power-law with $f_\lambda \propto \lambda^{-2}$ fitted in the range between 3800–5000 Å. **middle panel:** Residual spectrum after subtraction of the blue continuum shown together with the spectrum of the late M-dwarf Gliese 83.1 (M 4.5) scaled to match the strength of the observed TiO features. **lower panel:** The spectrum after the removal of the contribution of the secondary star. It exhibits broad emission features at 5500 and 7400 Å, tentatively identified as 3rd and 4th harmonic of the cyclotron fundamental. The solid line represents our favoured modell with $B = 52$ MG, $\theta = 80^\circ$ and for $kT = 10$ keV. The alternative interpretation for an $B = 41$ MG field is also given (dashed line).

demonstrated that absorption features from the illuminated side of the secondaries in magnetic CVs can be heavily suppressed due to the strong X/UV irradiation from the accretion region. We therefore caution that the distance derived from our single spectrum with unknown viewing geometry of the binary system can serve as an upper limit only.

4.3. A magnetic field estimate

After subtraction of a suitably scaled spectrum of Gl 83.1 two broad emission humps at $\lambda\lambda$ 5500 and 7400 Å clearly stand out in the red part of the spectrum (Fig. 4, lower panel), which we tentatively identify as cyclotron lines from the hot optically thin post-shock region.

An unambiguous estimate of the magnetic field strength is difficult to achieve with only two distinct humps observed. Their separation favours an interpretation as the 3rd and 4th harmonic of the cyclotron fundamental, in which case the field strength is 52±2 MG slightly depending on the plasma temperature and the yet unknown field orientation. An alternative interpretation as the 4th and 5th harmonics, in which case B is ~ 41 MG, cannot not completely excluded but results in a distinct mismatch of the expected humps with the shape of the continuum between

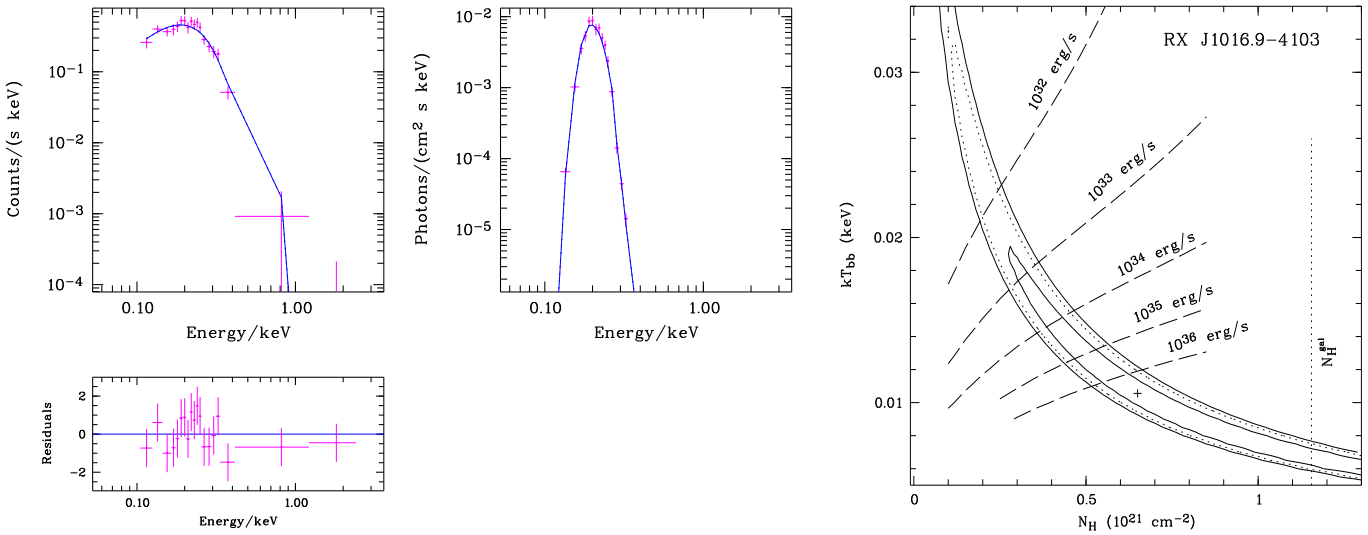

Fig. 5. Left: Phase-averaged X-ray spectrum of the two merged PSPC observations of RX J1016 unfolded with the sum of a blackbody and a thermal bremsstrahlung spectrum with a temperature fixed at 20 keV (see text for details). The lower left panel shows the residua of the fit in units of σ. **Right:** The 68%, 90% and 95% significance contours of the blackbody model fit to the merged PSPC spectrum of RX J1016 in the $N_{\rm H} - kT$ plane. Overplotted are the lines of constant luminosity in units of (D /100 pc)^2 (dashed), as well as the value of the total galactic absorbing column (vertical dotted line) according to Dickey & Lockman (1990).

6000–7000 Å. Normalized cyclotron absorption coefficients for both cases assuming $\theta = 80°$ and $kT = 10$ keV shown in Fig. 4 illustrate this ambiguity.

5. The X-ray spectrum

The two pointed PSPC observations have resulted in the detection of nearly 800 photons thus enabling spectral investigation. For the spectral analysis the source photons of the two PSPC pointings were merged and then extracted with a radius of 1′.5. The background was chosen from concentric circles around the source region with a radius of 3′. Other nearby sources were cut out, and the background area normalized to the source extraction area before the background subtraction. Standard corrections were applied using the dedicated EXSAS software package (Zimmermann et al. 1994). As a first step, we have considered the total spectrum as collected during each of the two observations (after merging). Adopting a blackbody plus a thermal bremsstrahlung model (the temperature of the latter fixed to 20 keV) we find that there is no need at all for the inclusion of the bremsstrahlung component, that is the spectral fit does not require any spectral component for hard emission (Fig. 5). The resulting best-fit temperature of the blackbody component is 10±7 eV and the absorbing column $N_{\rm H}$=6.4×10^{20} cm^{-2}, e.g. about 50% of the total galactic absorbing column in this direction (Dickey & Lockman 1990). However, this gives an unrealistic high luminosity for a cataclysmic variable due to the very low temperature. If we fix the temperature at the canonical value of 20 eV, the best-fit absorbing column is only $N_{\rm H}$=2.4×10^{20} cm^{-2}. The difference in reduced χ^2 is only marginal for all temperatures in the 10–25 eV range.

As a second step we have investigated the emission during the off-state phase intervals which has been observed for a total of 7340 sec. Selecting time intervals where the 60 sec averaged X-ray intensity is less than 0.05 cts/s, we find that the residual emission is consistent with being background radiation. The mean count rate during the X-ray bright phase (at >0.05 cts/s) is 0.38 cts/s in the PSPC.

Considering only the X-ray bright phase, the unabsorbed fluxes of the two model components in the ROSAT band (0.1–2.4 keV) are $F_{\rm bbdy}$ = 5.1×10^{-11} erg cm^{-2} s^{-1} (using kT$_{\rm bbdy}$=20 eV for comparison purposes) and $F_{\rm thbr}$ <9.8×10^{-13} erg cm^{-2} s^{-1}, giving a small flux ratio of $F_{\rm thbr}/F_{\rm bbdy} < 0.02$. The mean bolometric luminosity during the X-ray bright phase is (again with kT$_{\rm bbdy}$=20 eV) $L_{\rm X}$ = 2.4×10^{32} (D / 100 pc)^2 erg/s.

6. Discussion and conclusion

The measured period of $P = 134$ min places RX J1016 in the 2–3 hr CV period gap which is thought to be due to the transition from orbital angular momentum loss by magnetic braking (P> 3 hr) to gravitational radiation (P< 2 hr) (King 1988). Over the last years, more polars have been found with periods in the 2–3 hr range thus re-initiating the debate on the existence and significance of the period gap for magnetic systems (Wickramasinghe & Wu 1994, Wheatley 1995).

The shape of the X-ray light curve strongly argues for a self-eclipsing polar. The length of the X-ray bright phase of $\lesssim 0.5$ phase units suggests (within our limited accuracy) an one pole accreting geometry such that the accretion region passes behind the limb of the white dwarf for half the orbital period. The lack of eclipses implies $i < 78°$.

Our tentative estimate of the magnetic field strength is 52±2 MG and the strong soft X-ray excess are in good

agreement with the correlation found between these quantities (Beuermann 1998).

The strongly modulated soft X-ray emission, the seemingly synchronous rotation, the strength and relative intensities of the Balmer and He II emission lines as well as the cyclotron humps in the optical spectrum clearly suggest the polar nature of RX J1016 though no polarimetric measurements have been made. More detailed optical photometry and phase-resolved spectroscopy as well as polarimetry are needed to determine the system parameters of this new polar.

Acknowledgements. We thank R. Egger for help during the ESO observing run and A.D. Schwope for generously providing help and software for the cyclotron spectroscopy. JG and RS are supported by the Deutsches Zentrum für Luft- und Raumfahrt (DLR) GmbH under contract No. FKZ 50 QQ 9602 3 and 50 OR 9206 8. The ROSAT project is supported by the German Bundesministerium für Bildung, Wissenschaft, Forschung und Technologie (BMBF/DLR) and the Max-Planck-Society.

References

Bailey J., 1981, MNRAS 197, 31
Beuermann K., Burwitz V., 1995, ASP Conf. Ser. 85, 99
Beuermann K., 1998, in Perspectives of High Energy Astronomy & Astrophysics, Proc. of Int. Coll. to commemorate the Golden Jubilee of TIFR, Tata Inst. of Fund. Research, India, Aug. 1996, p. 100
Beuermann K., Weichhold M., 1998, A&A (in press)
Burwitz V., Reinsch K., Schwope A.D., et al., 1996, A&A 305, 507
Davey S.C., Smith R.C., 1996, MNRAS 280, 481
Dickey J.M., Lockman F.J., 1990, ARA&A 28, 215
Greiner J., Remillard R., Motch C., 1995, in Cataclysmic Variables, eds. A. Bianchini, M. Della Valle, M. Orio, ASSL 205, p. 161
Greiner J., 1996, in Supersoft X-ray Sources, ed. J. Greiner, Lecture Notes in Physics 472, Springer, p. 285
Greiner J., Remillard R., Motch C., 1998, A&A 336, 200
Greiner J., Schwarz R., Wenzel W., 1998, MNRAS 296, 437
King A.R., 1988, QJRAS 29, 1
Kirkpatrick J.D., McCarthy D.W., 1994, AJ 107, 333
Kujpers J., Pringle J.E., 1982, A&A 114, L4
Leggett S.K., 1992, ApJS 83, 351
Mateo M., Schechter P., 1989, 1st ESO/ST-ECF Data Analysis Workshop, eds. Grosbol P.J., Murtagh F. & Warmels R.H., p. 69
Patterson J., 1984, ApJS 54, 443
Schwarz R., Schwope A.D., Beuermann K., et al. , 1998, A&A 338, 465
Schwarzenberg-Czerny A., 1989, MNRAS 241, 153
Schwope A.D., Beuermann K., Catalán M.S., Metzner A., Steeghs D., 1998, MNRAS (subm.)
Stellingwerf R.F., 1978, ApJ 224, 953
Warner B., 1995, Cataclysmic Variable Stars, Cambridge Univ. Press, Cambridge
Wheatley P.J., 1995, MNRAS 274, L51
Wickramasinghe D.T., Wu K., 1994, ApSS 211, 61
Woelk U., Beuermann K., 1996, A&A 306, 232
Zimmermann H.U., Becker W., Belloni T., et al., 1994, MPE report 257